—Communication—

Preparation and Cycle Characteristics of Nano-Crystalline $Li_xFe_yO_z$ with Amorphous Structure

Y.T. LEE,[a] Y. S. LEE,[b] Y. SATO,[c] K. KOBAYAKAWA,[c] and Y. K. SUN[a]*

[a]Department of Chemical Engineering, Hanyang University (17 Haengdang-dong, Seoul 133-791, Korea)
[b]Department od Applied Chemical Engineering, Chonnam National University (300 Youngbong-dong, Gwangju 500-756, Korea)
[c]Department of Applied Chemistry, Kanagawa University (3-27-1 Rokkakubashi, Kanagawa-ku, Yokohama 221-8686, Japan)

Received May 19, 2003 ; Accepted August 28, 2003

Lithium iron oxides ($Li_xFe_yO_z$) were synthesized using LiOH and α-FeOOH by the solid-state reaction at various temperatures (200-800℃). The lithium iron oxide obtained at 200℃ showed an amorphous nano-crystalline phase in the XRD diagram. It presented not only a high initial discharge capacity (215 mAh g^{-1}), but also excellent cycle retention from the 11th to the 50th cycle (95%) between 1.5 V and 4.5 V. However, the powder obtained at 800℃ showed a single α-$LiFeO_2$ phase and exhibited very poor cycle performance below 5 mAh g^{-1} under the same test condition.

Key Words : Lithium Iron Oxides, Solid-state Method, Structural Transformation, Spinel $LiFe_5O_8$, Tetragonal $LiFeO_2$

1 Introduction

Lithium iron oxides are very prospective cathode materials compared to other layered cathode materials based on their environment and cost aspects. It is well known that $LiFeO_2$ has different forms, *i.e*, the α-, β-, γ-, and conjugated forms, due to the synthetic conditions and synthetic methods. The α-$LiFeO_2$ is a cubic unit cell of space group $Fm3m$, and β-$LiFeO_2$ (monoclinic, C $2/c$) is formed by an intermediate phase during the ordering process. The γ-$LiFeO_2$ (tetragonal, $I4_1/amd$) is obtained by reducing the symmetry from cubic to tetragonal by ordering the Li^+ and Fe^{3+} ions at octahedral sites.[1-9]

Recently, Tabuchi *et al*. reported a new form of metastable lithium iron oxides ($Li_{1-x}Fe_{5+x}O_8$), which has been synthesized using α-$NaFeO_2$ and LiCl in ethanol by the solvothermal reaction at low temperature (220℃). They revealed that this lithium iron oxide is formed as a solid solution, which is composed of Fe_3O_4 ($Fd\bar{3}m$, a = 8.396 Å) and β-$LiFe_5O_8$ ($Fd\bar{3}m$, a = 8.333 Å), using various analysis techniques. They also announced that the oxidation state of lithium iron oxide was reduced from 3+ during a long synthetic process, however, the moving of Fe^{3+} ions to tetrahedral sites in a ccp oxygen array disturbed the easy preparation of the lithium iron oxide.[7]

Furthermore, Kim *et al*. reported that nano-crystalline lithium iron oxide ($Li_xFe_yO_z$) with amorphous type presented a high discharge capacity of about 140 mAh g^{-1} with a fairly good cycleability in the range of 1.5 and 4.3 V. They have synthesized various kinds of lithium iron oxides with the Li/Fe ratio of 0.69-1.22 using the solution method, which utilized the oxidation reaction of Fe^{2+} with lithium peroxide in the presence of excess lithium hydroxide in aqueous medium. Although they successfully obtained the lithium iron oxide with a fairly good battery performance at low temperature (200℃), the cycle characteristics and synthetic method, due to the excess use the lithium source by the solution method, are still unsatisfactory aspects for use as a practical cathode material for lithium secondary batteries.[10]

On the basis of above reports, it was initiated in order to easily synthesize a new type of lithium iron oxide with an excellent cycle performance using a solid-state method. We report the synthesis and electrochemical characteristics of the amorphous type of nano-crystalline $Li_xFe_yO_z$, which was obtained at various calcination temperatures.

2 Experimental

Lithium iron oxide was synthesized using $LiOH \cdot H_2O$, α-FeOOH under N_2 atmosphere by solid-state method. The stoichiometric amounts (Li/Fe = 1.0) of starting materials were thoroughly grounded in a mortar for 1 h. The mixture was precalcined at 100℃ for 12 h and then ground again in a mortar for 30 min. The intermediate powder was pressed into a pellet and it was calcined at various temperatures (200-800℃) for 12 h under N_2 atmosphere. The powder X-ray diffraction using Cu-Kα radiation was used to identify the crystalline phase of the synthesized materials and cycled electrodes. The particle size and morphology of the compounds were observed using a field emission scanning electron microscope.

The electrochemical characterization was performed using CR2032 coin-type cell. The cathode was fabricated with 20 mg of accurately weighed active material and 12 mg of conductive binder (8 mg of Teflonized acetylene black (TAB) and 4 mg of graphite). It was pressed on 200 mm^2 stainless steel mesh used as the current collector under a pressure of 300 kg cm^{-2} and dried at 150℃ for 5 h in an vacuum oven. The test cell was made of a cathode and a lithium metal anode (Cyprus Foote Min-

eral Co.) separated by a porous polyethylene (PE) film. The electrolyte used was a mixture of 1 M $LiPF_6$-ethylene carbonate (EC)/dimethyl carbonate (DMC) (1 : 2 by vol., Ube Chemicals, Japan). The charge and discharge current density was 0.1 mA cm^{-2} with a cut-off voltage of 1.5 to 4.5 V at room temperature (25℃).

3 Results and Discussion

Figure 1 shows the X-ray powder diffraction (XRD) of the resulting powders calcined at various temperatures. The lithium iron oxide obtained at 200℃ (Fig. 1(a)) showed a broad reflection pattern with amorphous type, which was made up of polymorphous structures of the amorphous spinel-like and a trace of cubic α-$LiFeO_2$. Indeed, it is very difficult to detect its critical structure only within the XRD pattern, due to the low crystallinity and some impurities over the whole scan range. The XRD pattern obtained at 400℃ exhibited stronger α-$LiFeO_2$ main diffraction peaks, such as (111), (200), and (220), than those of the 300℃ sample. Moreover, the compound obtained at 800℃ exhibited an ideal single α-$LiFeO_2$ cubic phase, which is well known to be very difficult to insert/ extract lithium into and out of its structure.

The morphologies of the powders obtained at various temperatures were observed using a scanning electron microscope. The powder obtained at 200 and 300℃ had nano-crystallite sizes as shown in Fig. 2(a), which are composed of small particle sizes of about 20-50 nm. On the other hand, the α-$LiFeO_2$ powder obtained at 800℃ showed fairly increased particle sizes about 700-800 nm and a slightly changed particle shape. It is noticeable that the average particle size of the powder at 800℃ was 20 times larger as that of the powder obtained at 200℃.

Figure 3 shows the charge/discharge curves of the Li/

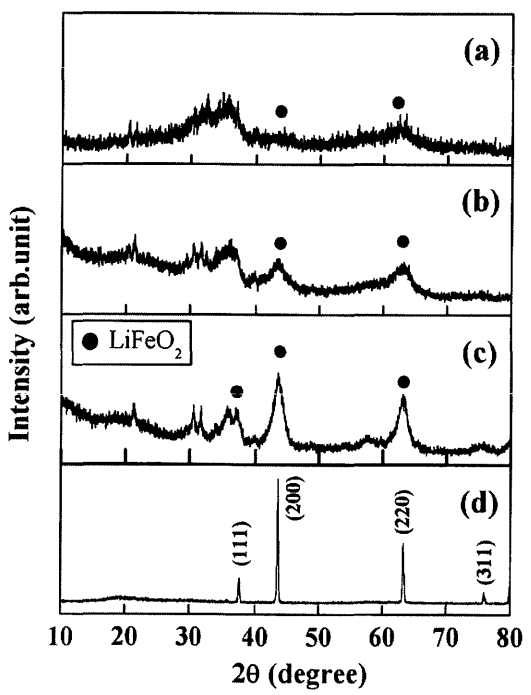

Fig. 1 X-ray diffraction patterns for $Li_xFe_yO_z$ powders obtained at (a) 200℃, (b) 300℃, (c) 400℃, and (d) 800℃.

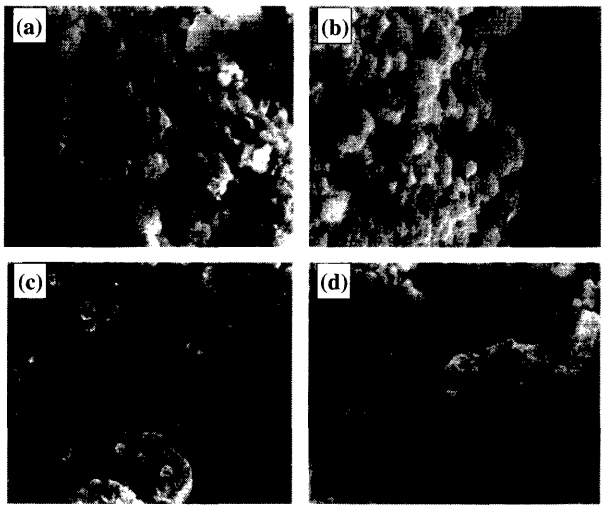

Fig. 2 Scanning electron microscopes of $Li_xFe_yO_z$ powders obtained at (a) 200℃, (b) 300℃, (c) 400℃, and (d) 800℃.

$Li_xFe_yO_z$ cells obtained at various calcination temperatures. The first charge curve of the Li/$Li_xFe_yO_z$ obtained at 200℃ (Fig. 3(a)) rapidly increased up to 4.0 V. This cell shows a small plateau region at about 4.1 V and exhibits another long voltage plateau between 4.2 and 4.3 V. While the first discharge curve drastically decreased to 3.3 V, it showed two small voltage plateaus between 2.0 and 1.5 V. For the second cycle, the voltage profile gradually decreased without any remarkable voltage plateau and exhibited a slightly different shape compared to that of the first cycle. The Li/$Li_xFe_yO_z$ cell obtained at 300℃ (Fig. 3(b)) showed a very similar discharge profile compared to that of sample obtained at 200℃.

On the other hand, the Li/$Li_xFe_yO_z$ cell obtained at 400℃ exhibited a couple of different electrochemical characteristics compared to those of the lithium iron oxides obtained at lower temperatures (200℃ and 300℃). First, this cell shows a very small discharge capacity compared to those obtained at lower temperatures. Second, there is no voltage plateau in the first discharge curve. It showed a smooth voltage profile until 1.5 V and no voltage plateau below 2.0 V as mentioned above. Lastly, this cell shows an increase in the discharge capacity upon cycling, although the amount of the increase is very small. These unique indications as shown in Fig. 3(c) suggest that the lithium iron oxide obtained at 400℃ has a very different characteristic compared to those obtained at the lower temperatures. We suspect that the main reason for these unique characteristics is due to the growth of the $LiFeO_2$ (β- or γ-form) phase at 400℃.[11] Moreover, the lithium iron oxide obtained at 800℃ shows a very small discharge capacity of 5 mAh g^{-1} after 50 cycles. This small initial discharge capacity supports the phase transformation from β (or γ)-$LiFeO_2$ into the inactive α-$LiFeO_2$ material at high temperature (800℃). Therefore, we expect that the amount of the electrochemically active amorphous structure gradually decreased as the calcination temperature increases, which induced an abrupt capacity decrease in the initial discharge capacity of the lithium iron oxide system.

Figure 4 shows the variation in the specific discharge

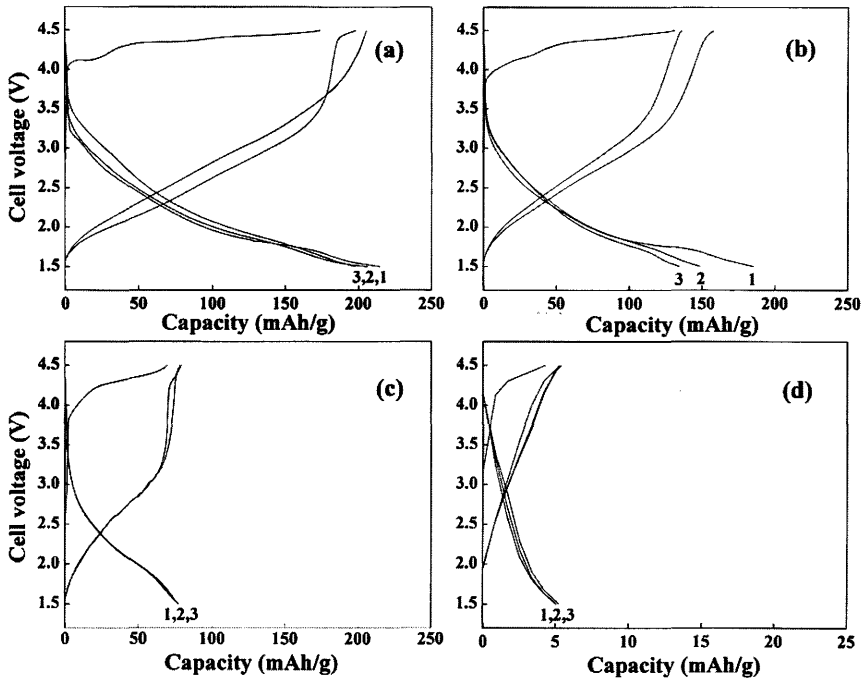

Fig. 3 Charge/discharge curves of $Li_xFe_yO_z$ powders prepared at (a) 200℃, (b) 300℃, (c) 400℃, and (d) 800℃. The test condition was a current density of 0.1 mA cm^{-2} between 1.5 and 4.5 V at room temperature.

capacity with the number of cycles for the lithium iron oxide materials obtained at various temperatures. The charge/discharge current density was 0.1 mA cm^{-2} with a cut-off voltage of 1.5 to 4.5 V at room temperature. The lithium iron oxide obtained at 200℃ presents the highest initial discharge capacity of 215 mAh g^{-1} and an excellent cycle retention from the 11th to the 50th cycle. Although this material showed a large capacity loss until the 10th cycle, the cycle retention rate from the 11th to 50th cycle was 95%, which is the highest value as previously reported. It has been considered that the powder obtained at 200℃ with a smaller particle size, especially nano- crystallite size, could exhibit a high discharge capacity (with higher specific surface area) and a good structure stability by reducing the volume expansion during the lithium insertion/extraction.[10,12,13]

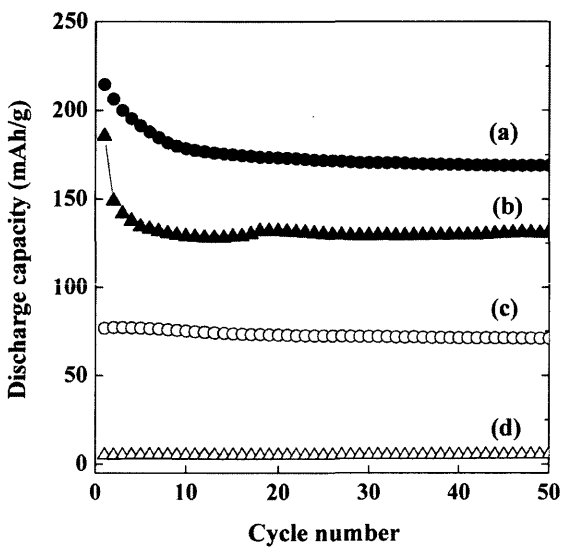

Fig. 4 Discharge capacity vs. number of cycles for Li/$Li_xFe_yO_z$ cells obtained at (a) 200℃, (b) 300℃, (c) 400℃, and (d) 800℃.

In order to investigate a structural change during cycling, especially in the initial stage, *ex-situ* XRD and a transmission electron microscopy (TEM) analysis conducted on the same electrodes after at various cycles. Unfortunately, we failed to get a concrete result, which could clearly show the structural changes from the 1st cycle to 50th cycle. It is very difficult to detect that the particles on the electrode after the 50th cycle were broken due to the lithium insertion/extraction during long-term cycling because it was originally an amorphous phase with a small nano-particle size (20-40 nm). It is considered that the phase confirmation of lithium iron oxide needs to investigate at each step using magnetic property tools, such as magnetic field dependence of magnetization (*M-H*) data. Further work involving the transformation mechanism is now in progress and these results will be reported elsewhere.

4 Conclusion

Lithium iron oxides, $Li_xFe_yO_z$, have synthesized using $LiOH \cdot H_2O$ and α-FeOOH by solid-state method at various temperatures (200-800℃). Nano-crystalline lithium iron oxides obtained at 200℃ showed a high initial discharge capacity (215 mAh g^{-1}) and an excellent cycle retention at room temperature, although it exhibited a gradual capacity decrease until the 10th cycle. It was found that the decrease in the initial capacity of the Li/$Li_xFe_yO_z$ cells resulted from the growth of inactive α-$LiFeO_2$ material at high temperature (800℃).

Acknowledgement

This work is supported in part by the Ministry of Information & Communication of Korea ("Support Project of

University Information Technology Research Center" supervised by KIPA).

References

1) R. Kanno, T. Shirane, Y. Kawamoto, Y. Takeda, M. Takano, M. Ohashi, and Y. Yamaguchi, *J. Electrochem. Soc.*, **146**, 2435 (1996).
2) T. Shirane, R. Kanno, Y. Kawamoto, Y. Takeda, M. Takano, T. Kamiyama, and F. Izumi, *Solid State Ionics*, **79**, 227 (1995).
3) M. Tabuchi, K. Ado, H. Sakaebe, C. Masquelier, H. Kageyama, and O. Nakamura, *Solid State Ionics*, **79**, 220 (1995).
4) M. Tabuchi, C. Masquelier, T. Takeuchi, K. Ado, I. Matsubara, T. Shirane, R. Kanno, S. Tsutsui, S. Nasu, H. Sakaebe, and O. Nakamura, *Solid State Ionics*, **90**, 129 (1996).
5) K. Ado, M. Tabuchi, H. Kobayashi, H. Kageyama, O. Nakamura, Y. Inaba, R. Kanno, M. Takagi, and Y. Takeda, *J. Electrochem. Soc.*, **144**, L 177 (1997).
6) M. Tabuchi, S. Tsutsui, C. Masquelier, R. Kanno, K. Ado, I. Matsubara, S. Nasu, and H. Kageyama, *J. Solid State Chem.*, **140**, 159 (1998).
7) M. Tabuchi, K. Ado, H. Kobayashi, I. Matsubara, H. Kageyama, M. Wakita, S. Tsutsui, S. Nasu, Y. Takeda, C. Masqulier, A. Hirano, and R. Kanno, *J. Solid State Chem.*, **141**, 554 (1998).
8) Y. Sakurai, H. Arai, S. Okada, and J. Yamaki, *J. Power Sources*, **68**, 711 (1997).
9) Y. Sakurai, H. Arai, and J. Yamaki, *Solid State Ionics*, **113-115**, 29 (1998).
10) J. Kim and A. Manthiram, *J. Electrochem. Soc.*, **146**, 4371 (1999).
11) H. Arai, S. Okada, Y. Sakurai, and J. Yamaki, *Solid State Ionics*, **95**, 275 (1997).
12) A. Manthiram and C. Tsang, *J. Electrochem. Soc.*, **143**, L 143 (1996).
13) C. Tsang and A. Manthiram, *J. Electrochem. Soc.*, **144**, 520 (1997).